

Ride Quality Improvements by Means of Numerical Optimization Techniques

Giovanni Mengali*
University of Pisa, 56126 Pisa, Italy

A numerical optimization technique is employed to obtain an idealized model for the dynamics of an aircraft, with an aim at improving its ride quality characteristics. The object function to be minimized in the optimization process is a quadratic performance index, representing the mean-square acceleration level experienced by the vehicle in its flight in an atmospheric turbulence field. Handling quality requirements are taken into account by means of suitable side constraints on the eigenvalues and eigenvectors of the aircraft model. The idealized model, resulting from the minimization process, can be effectively used as a model to be followed by a control system. A numerical example, based on two-degree-of-freedom longitudinal dynamics of a jet transport, is discussed.

Introduction

ONE of the most important areas of employment of active control systems is the study of flight in atmospheric turbulence. This study involves many different aspects of the aircraft development (e.g., fatigue damage, transient peak loads, handling quality, and ride comfort), which are often strictly connected. As a consequence, the project must outline strategies that reflect this state of things.¹ In particular, in this work we are interested in pointing out the interaction between handling and riding qualities.²

Ride quality is related to a number of factors, but especially to aircraft dynamics. One of the most important parameters is the level and duration of the root-mean-square accelerations experienced by an aircraft in its flight in atmospheric turbulence. Since human tolerance to vibration exposure is very poor, it is necessary to limit vertical and lateral accelerations (especially at some critical fuselage stations) so as to obtain good comfort levels for crew and passengers.³

An important contribution to improving aircraft performance comes from complete knowledge of the physical parameters that characterize the ride quality performance and its sensitivity to parameter variations. To this end the aircraft must be investigated in terms of its free response, which is governed by the eigenstructure of the vehicle's dynamic model or by the set of its eigenvalues and eigenvectors. In this paper we look for the optimal model (the one attaining the best ride quality level) by modifying its eigenstructure within the constraints imposed by handling quality requirements.

We proceed as follows. A scalar quadratic criterion is first defined to quantify the ride quality performance of the aircraft model [or system model (SM)] in atmospheric turbulence. Then an idealized model (IM), corresponding to the minimization of the above criterion, is found that satisfies given constraints on the model eigenvalues and eigenvectors. This approach allows us: (i) to gauge the influence of a change in each eigenvalue and/or eigenvector component and (ii) to quantitatively measure both the "distance" between the SM and IM and the maximum attainable improvement in ride quality performance. A simple control law, minimizing the mean-square difference between the SM and IM according to an implicit model-following technique, is also used for some comparative results.

System Model

The aircraft dynamics are described by the following linear, time-invariant system:

$$\dot{x} = A_0x + B_0u + E_0w_g \quad (1)$$

$$y = C_0x + D_0u + W_0w_g \quad (2)$$

Equations (1) and (2) describe the SM. Here $x \in R^n$ denotes the state of the system, $u \in R^m$ indicates the input (or control) variable, $w_g \in R^r$ contains the gust velocity components, and $y \in R^p$ is the output variable. All x, u, w_g, y are functions of time t .

Since we are concerned with the reduction of the acceleration level experienced by the aircraft in its flight in an atmospheric turbulence field, we choose y to be composed by signals from accelerometers placed in suitable stations along the vehicle fuselage.

The atmospheric turbulence is modeled by a linear system driven by white noise,

$$\dot{d}_g = F_0d_g + G_0\eta_g \quad (3)$$

$$w_g = H_0d_g \quad (4)$$

where $d_g \in R^s$ denotes the states of the atmospheric disturbances and $\eta_g \in R^q$ is white noise with constant intensity. The matrices in (3) and (4) are assigned according to a Dryden model. Defining

$$\xi \equiv \begin{bmatrix} x \\ d_g \end{bmatrix} \quad (5)$$

with $\xi \in R^{n+s}$, Eqs. (1–4) reduce to

$$\dot{\xi} = A\xi + Bu + G\eta_g \quad (6)$$

$$y = C\xi + Du \quad (7)$$

where

$$A \equiv \begin{bmatrix} A_0 & E_0H_0 \\ 0 & F_0 \end{bmatrix}, \quad B \equiv \begin{bmatrix} B_0 \\ 0 \end{bmatrix}, \quad G \equiv \begin{bmatrix} 0 \\ G_0 \end{bmatrix} \\ C \equiv [C_0 \quad W_0H_0], \quad D \equiv D_0 \quad (8)$$

The aircraft longitudinal and lateral normal acceleration components have the following expressions:

$$a_{z_j} = \dot{w} - U_0q - l_j\dot{q} + \sum_i \Phi_{z_i}(l_j)\ddot{\eta}_{z_i} \quad (9)$$

$$a_{y_j} = \dot{v} + U_0r - g\phi + l_j\dot{r} + \sum_i \Phi_{y_i}(l_j)\ddot{\eta}_{y_i} \quad (10)$$

where v and w are side-to-side and vertical velocity components, q and r are pitch and yaw rate, ϕ is the roll angle, g is the acceleration of gravity, U_0 is the steady-state velocity of the aircraft, Φ_{y_i} and Φ_{z_i} are the bending mode displacement coefficients with generalized coordinates η_{y_i} and η_{z_i} , and l_j is the distance (with sign) between the generic accelerometer and the aircraft center of gravity (CG).

Received Aug. 8, 1992; revision received May 20, 1993; accepted for publication Nov. 13, 1993. Copyright © 1994 by the American Institute of Aeronautics and Astronautics, Inc. All rights reserved.

*Research Scientist, Department of Aerospace Engineering.

Here l_j is positive when the sensor is placed forward of the aircraft's CG. Also, the summations in Eqs. (9) and (10) are extended to all the generalized coordinates taken into account.

Aircraft Performance in Atmospheric Turbulence

What we need is a performance index PI representing the "measure" of the aircraft performance in atmospheric turbulence. Since there are many practical advantages in using a quadratic PI, we choose the mean-square acceleration level. Accordingly, we define

$$PI \equiv E\{y^T W_y y\}/p \quad (11)$$

where $E\{\cdot\}$ is the expectation operator, W_y is a given nonnegative-definite symmetric weighting matrix, and p represents the number of accelerometers along the fuselage.

We first consider the PI evaluation in the case of the free SM (i.e., open-loop SM). In other words we do not employ the control vector u to modify the aircraft dynamics, and accordingly, we suppose $u = 0$ in Eqs. (1) and (2). Bearing in mind Eq. (7), we obtain

$$E\{y^T W_y y\}/p = E\{\xi^T C^T W_y C \xi\}/p = \text{tr}(C^T W_y C E\{\xi \xi^T\})/p \quad (12)$$

where $\text{tr}(\cdot)$ is the trace operator. It is known that $E\{\xi \xi^T\}$, the covariance matrix of ξ , can be obtained as the solution of the following linear equation (see Ref. 4, pp. 328–334):

$$A E\{\xi \xi^T\} + E\{\xi \xi^T\} A^T + G G^T = 0 \quad (13)$$

Formula (13) is a standard Lyapunov equation for which efficient numerical methods, as for example the Bartels-Stewart algorithm,⁵ are available.

In summary, PI can be evaluated from Eqs. (12) and (13), where the matrices A , C and G are as given in Eqs. (6–8).

Idealized Model

The following questions are of interest: (i) Is it possible to define an "optimum" behavior (in terms of aircraft ride quality) for an aircraft in atmospheric turbulence? (ii) If so, which is the best attainable performance and which are the parameters that chiefly influence this performance? To answer these questions, we introduce the aircraft IM, which has the structure

$$\dot{x}_m = \hat{A} x_m + E_0 w_g \quad (14)$$

$$y_m = \hat{C} x_m + W_0 w_g \quad (15)$$

along with the disturbance model (3) and (4). We assume that x_m and y_m have the same dimensions of x and y . Equations (14) and (15) may also be written as

$$\dot{\xi}_m = A_m \xi_m + G \eta_g \quad (16)$$

$$y_m = C_m \xi_m \quad (17)$$

where

$$A_m \equiv \begin{bmatrix} \hat{A} & E_0 H_0 \\ 0 & F_0 \end{bmatrix}, \quad G \equiv \begin{bmatrix} 0 \\ G_0 \end{bmatrix}, \quad C_m \equiv [\hat{C} \quad W_0 H_0] \quad (18)$$

In analogy with (11), the IM performance is evaluated by means of the following PI:

$$E\{y_m^T W_y y_m\}/p = E\{\xi_m^T C_m^T W_y C_m \xi_m\}/p = \text{tr}(Q_m X_m)/p \quad (19)$$

where

$$X_m \equiv E\{\xi_m \xi_m^T\} \quad (20)$$

$$Q_m \equiv C_m^T W_y C_m \quad (21)$$

In Eq. (18), matrices \hat{A} and \hat{C} must be chosen according to some criterion. They are the unknowns of our problem and completely define the IM. On the other hand, since the entries of \hat{C} are linear functions of the entries of \hat{A} [as a consequence of Eqs. (9) and (10)], we conclude that \hat{A} is the only unknown here.

From a practical point of view, \hat{A} cannot be employed as an ordinary matrix, for it must contain the main characteristics of the physical system we want to represent. Indeed, the IM eigenstructure must be suitably chosen so as to warrant that the IM dynamics reflects the airplane dynamics. In other words we must choose the IM in such a way that its eigenvalues and eigenvectors can only vary within pre-established boundaries. The constraints we impose on the eigenstructure of \hat{A} may be chosen according to the handling quality specifications. In this way a good dynamic response of the free IM is guaranteed. In summary the problem can be approached as follows: minimize the PI defined by Eq. (19) as a function of \hat{A} with specified constraints on the eigenvalues and eigenvectors of \hat{A} .

Optimization Procedure

Without loss of generality we assume that the eigenvalues of \hat{A} are distinct (in this hypothesis M_b , the modal matrix of \hat{A} , is nonsingular). Using a spectral decomposition for \hat{A} we obtain

$$\hat{A} = M_b \Lambda_b M_b^{-1} \quad (22)$$

where Λ_b is the block-diagonal matrix

$$\Lambda_b = \begin{bmatrix} \ddots & 0 & 0 \\ 0 & \Lambda_j & 0 \\ 0 & 0 & \ddots \end{bmatrix}, \quad j = 1, \dots, N \quad (23)$$

and $N = n_{re} + \frac{1}{2}n_{im}$. Also, n_{im} and n_{re} are the number of the complex and real eigenvalues. Denoting with $\rho_i \exp(\pm j\theta_i)$ the generic pair of complex eigenvalues, Λ_i in Eq. (23) becomes

$$\Lambda_i = \begin{bmatrix} \rho_i \cos \theta_i & \rho_i \sin \theta_i \\ -\rho_i \sin \theta_i & \rho_i \cos \theta_i \end{bmatrix} \quad (24)$$

Vice-versa for real eigenvalues we have

$$\Lambda_i = [\lambda_i] \quad (25)$$

It turns out that, as a consequence of the above representation of Λ_b , the entries of M_b are real valued. Furthermore, its columns are the real and imaginary parts of the eigenvectors of \hat{A} (if the corresponding eigenvalues are complex) or just the real eigenvectors (if the corresponding eigenvalues are real). The polar form for the complex eigenvalues allows us to take into account the constraints on IM in a simple way. In fact, flying quality requirements on the eigenvalues can be expressed as follows⁶

$$\rho_i^{(\min)} \leq \rho_i \leq \rho_i^{(\max)}, \quad \theta_i^{(\min)} \leq \theta_i \leq \theta_i^{(\max)} \quad (26)$$

$$\lambda_i^{(\min)} \leq \lambda_i \leq \lambda_i^{(\max)} \quad (27)$$

where the superscripts *min* and *max* denote minimum and maximum values attained by the indicated variables.

Define

$$\nu^T \equiv (\rho_1, \theta_1, \rho_2, \theta_2, \dots, \lambda_1, \dots, \lambda_{re}) \quad (28)$$

and call μ the vector containing the columns of M_b (equivalently, the eigenvectors of \hat{A}). We observe that the PI to be minimized is a function of μ and ν . Thus, our problem may be formulated as follows: Find A_m [or \hat{A} , as a consequence of Eq. (18)] so as to minimize

$$f(\mu, \nu) \equiv \text{tr}(Q_m X_m)/p \quad (29)$$

with the constraints

$$A_m X_m + X_m A_m^T + G G^T = 0 \quad (30)$$

$$\mu_i^{(\min)} \leq \mu_i(\hat{A}) \leq \mu_i^{(\max)} \quad (31)$$

$$\nu_i^{(\min)} \leq \nu_i(\hat{A}) \leq \nu_i^{(\max)} \quad (32)$$

where the index i is now extended to only those components of μ and ν we want to change with respect to the initial configuration. In particular, bearing in mind that the eigenvectors are determined within multiplicative constants, only some of the components of μ will be modified.

The method of feasible directions⁷ is used to solve the above problem. This method employs first-order gradient information on objective function and constraints to determine a search direction and a scalar multiplier that reduce $f(\mu, \nu)$ while maintaining a feasible design. In Appendix I it is shown that the gradient of $f(\mu, \nu)$ can be obtained in closed form.

Control Law

We remark that the process outlined above gives useful information both on the performance of the free SM as compared to the "best" attainable IM and on the physical parameters that chiefly influence such a performance. Unfortunately, it does not answer the question of how we can modify the SM in order to closely follow the IM behavior. Although this is a crucial aspect of the problem, in the sequel we just modify the SM by means of a simple control law.

A wide class of control techniques is based upon the implicit model-following idea^{8,9}. This technique appears to be a natural choice in the present problem, for we aim at forcing the SM to follow IM dynamics in the best possible way.

We make use of a quadratic criterion, i.e., we minimize

$$J = (\dot{x}_m - \dot{x})^T R (\dot{x}_m - \dot{x}) - u^T T u \quad (33)$$

where R and T are nonnegative-definite symmetric matrices. The former weights the differences between the derivatives of the IM and SM states whereas the latter weights the maximum values of the rotations of the control surfaces. In other words the differences between the IM and SM are minimized in a least square sense.

Minimization of Eq. (33) is straightforward, and following Markland,¹⁰ the result is found to be

$$u_{\text{opt}}(B_0^T R B_0 + T)^{-1} B_0^T R (\hat{A} - A_0)x = Kx \quad (34)$$

As is seen, the optimal control law u_{opt} is a full-state feedback control law. Substituting Eq. (34) into Eqs. (6–8), we obtain the controlled model (CM)

$$\dot{\xi} = A_c \xi + G \eta_g \quad (35)$$

$$y = C_c \xi \quad (36)$$

where

$$A_c = \begin{bmatrix} A_0 + B_0 K & E_0 H_0 \\ 0 & F_0 \end{bmatrix}, \quad (37)$$

$$C_c \equiv [C_0 + D_0 K \quad W_0 H_0]$$

Table 1 Open-loop characteristics of SM

Eigenvalues	Damping	Frequency,		μ_{α_r}/μ_{q_r}	μ_{α_i}/μ_{q_i}	PI, ft ² /s ⁴
		rad/s				
$-1.075 \pm j2.956$	0.3418	3.1455		0.3050	-0.3660	0.3112

Application of Theory

In this section some results obtained with the above-mentioned method are analyzed. We consider a simplified case, namely the two degree-of-freedom short-period longitudinal dynamics¹¹ of a DC-8-type jet transport. (The data used in this example have been extracted from McRuer, Ashkenas, and Graham¹¹ for the DC-8 aircraft, except those pertinent to the symmetric aileron deflections. The latter have been estimated by the author.) This vehicle is in cruise condition at 33,000 ft of altitude with a Mach number equal to 0.84. The matrices in Eqs. (1–4) are defined in Appendix II. We assume that elevators and the symmetric rotation of ailerons are used as control means. The elastic modes have been omitted to simplify the discussion, and accordingly, Eq. (9) contains only the rigid-body terms. Although this omission is not necessary in our theory, it can be interpreted as if the elastic modes were designed to have little or no effect over the rigid-body frequencies.

The state variables in the motion equations are the vertical velocity component w (or the incidence α , i.e., the ratio of w and the steady-state velocity U_0), and the pitch rate q . The characteristics of open-loop dynamics (in terms of eigenvalues and eigenvectors) and the PI in Eq. (11) are given in Table 1.

Note that in this case W_y in Eq. (11) is the identity matrix and that our results correspond to vertical and pitching gust velocities of 1 fps intensity. Also, the quantities μ in the table are the entries of the matrix M_b , i.e.,

$$M_b = \begin{bmatrix} \mu_{\alpha_r} & \mu_{\alpha_i} \\ \mu_{q_r} & \mu_{q_i} \end{bmatrix} \quad (38)$$

and the subscripts r and i stand for the real and imaginary parts of the complex eigenvectors.

Suppose now we want to obtain the IM for the above example. The constraints are summarized in Table 2.

We are concerned with three cases. Case 1, the most general one, is compared with cases 2 and 3 where only the eigenvalues (case 2) or the eigenvectors (case 3) are changed with respect to the free SM values. In this way the separate effects of eigenvalue or eigenvector changes on the PI [given by Eq. (19)] are quantified. The results are summarized in Table 3. Note that, in case 1, the IM has poles with moduli and phases quite larger than those in the SM. Also, an important improvement in ride quality performance is obtained: Indeed, the IM PI is reduced by 77.6%. Moreover we point out that the eigenvectors play a fundamental role in the present problem. This is evident from case 2 wherein only the eigenvalues are modified and the performance improvement is very limited.

Table 2 Constraints on eigenvalues and eigenvectors for cases analyzed

Case	Eigenvalues	Eigenvectors
Case 1	$1.3 \leq \rho \leq 4, 1.875 \leq \theta \leq \pi$	$-1 \leq \mu_{\alpha_r}/\mu_{q_r} \leq 1, -1 \leq \mu_{\alpha_i}/\mu_{q_i} \leq 1$
Case 2	$1.3 \leq \rho \leq 4, 1.875 \leq \theta \leq \pi$	0.3050 ^a , -0.3660 ^a
Case 3	3.1453, ^a 1.919 ^a	$-1 \leq \mu_{\alpha_r}/\mu_{q_r} \leq 1, -1 \leq \mu_{\alpha_i}/\mu_{q_i} \leq 1$

^aSame value as for SM.

Table 3 Results obtained for cases of Table 2

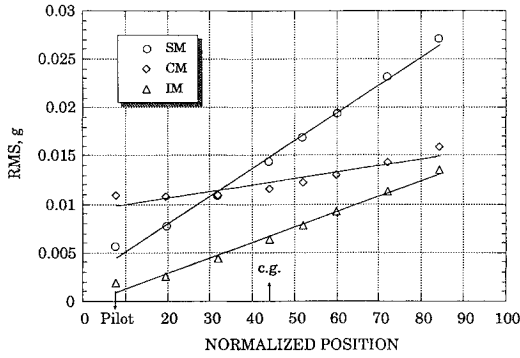
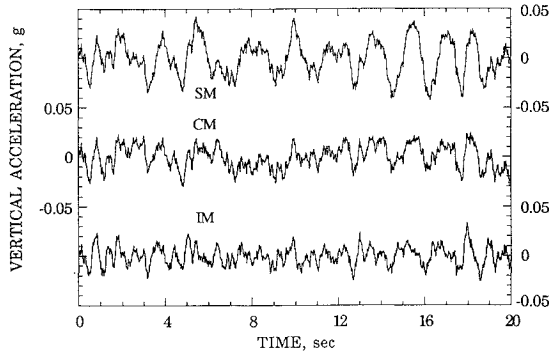
Case	Eigenvalues	Damping	Frequency,		μ_{α_r}/μ_{q_r}	μ_{α_i}/μ_{q_i}	PI, ft ² /s ⁴
			rad/s				
Case 1	$-3.999 \pm j0.007$	0.9999	4.0		-0.1734	-0.1744	0.0675
Case 2	$-0.873 \pm j2.7684$	0.3009	2.9027		0.3050	-0.3660	0.2845
Case 3	$-1.075 \pm j2.956$	0.3418	3.1455		0.2547	-0.3351	0.2280

Table 4 Comparisons between SM, CM, and IM

Model	Eigenvalues	Damping	Frequency, rad/s	μ_{α_r}/μ_{q_r}	μ_{α_i}/μ_{q_i}	PI, ft ² /s ⁴
SM	$-1.075 \pm j2.956$	0.3418	3.1455	0.3050	-0.3660	0.3112
CM	$-3.867 \pm j2.297$	0.8597	4.4988	-0.0421	-0.3377	0.1583
IM	$-3.999 \pm j0.007$	0.9999	4.0	-0.1734	-0.1744	0.0675

Table 5 State matrices for SM, CM, and IM

A_0	$A_0 + B_0 K$	\hat{A}
$\begin{bmatrix} -0.8060 & 824.2000 \\ -0.0107 & -1.3440 \end{bmatrix}$	$\begin{bmatrix} -0.9157 & 742.0164 \\ -0.0189 & -6.8198 \end{bmatrix}$	$\begin{bmatrix} -1.3045 & 386.4083 \\ -0.0188 & -6.6955 \end{bmatrix}$

**Fig. 1** Root-mean-square vertical acceleration along fuselage. Marks correspond to accelerometer positions, normalized to fuselage length.**Fig. 2** Comparison of simulated gust-induced accelerations at CG.

The IM results (case 1) are now compared with those corresponding to the CM. We assume that the matrices R and T in Eq. (33) are diagonal, so that J reduces to a weighted sum of squared terms. Thus, choosing the weights as the inverses of the maximum values of the weighted quantities (see Ref. 4, pp. 148–157), every term gives an equivalent contribution to J . Accordingly, we take

$$R = \text{diag}(1; 10,000), \quad T = \text{diag}(8100; 8100)$$

Here the R entries are computed considering as maximum values of w and q those taken at $t = 0$ when a step gust input is applied; vice-versa the T entries are chosen so as to limit the maximum rotation of the control surfaces to $\pm 4^\circ$. It has been obtained that

$$K = \begin{bmatrix} 1.3403 \times 10^{-3} & 8.1736 \times 10^{-1} \\ 1.7016 \times 10^{-3} & 1.4490 \times 10 \end{bmatrix}$$

The results are summarized in Tables 4 and 5.

Root-mean-square vertical accelerations along the fuselage are shown in Fig. 1, in which the SM, IM, and CM are compared. It appears that the acceleration levels at all the fuselage positions are minimum for the IM. On the other hand, the CM has a reduced slope in the acceleration curve, with a corresponding reduction in root-mean-square acceleration levels in those zones where this level is

more critical. Finally, it should be noted that the behavior of the SM qualitatively agrees with the experimental measurements reported in Sadoff et al.¹²

A more detailed description of the benefits provided by the CM is illustrated in Fig. 2, where simulated accelerations with the SM, CM, and IM at the CG of the aircraft are drawn vs time.

Conclusions

A numerical optimization technique has been discussed that improves the ride quality of an aircraft nominal configuration. This technique is based on the minimization of a quadratic performance index that characterizes the aircraft performance in atmospheric turbulence. Handling quality requirements are easily taken into account by imposing suitable side constraints on the eigenvalues and eigenvectors of the aircraft model. The above technique provides information on the following points: i) the parameters that chiefly influence ride quality, ii) the effects of an assigned percent variation of these parameters and iii) the open-loop performance and the “best” attainable performance of the aircraft. This information can be used to guide the vehicle arrangement and, possibly, for subsequent modifications of the system free response by means of control laws. In this second phase the IM, resulting from the optimization process, may be taken as the basis for a control law definition that exploits a model-following technique. Although the numerical examples deal only with a simple two-degree-of-freedom longitudinal dynamic model, they clearly show the potential of the described technique and the importance of the eigenvectors on the aircraft performance.

Appendix I: Computing Gradient of PI

Using a first-order optimization technique we compute the gradient of f in Eq. (29) with respect to the generic free parameter γ . According to Kwakernaak and Sivan,¹³ we obtain

$$\frac{\partial f}{\partial \gamma} = \frac{1}{p} \text{tr} \left(2U_m \frac{\partial A_m}{\partial \gamma} X_m + X_m \frac{\partial Q_m}{\partial \gamma} \right) \quad (\text{A1})$$

where X_m is given in Eq. (26) and U_m is the matrix solution of the Lyapunov equation

$$A_m^T U_m + U_m A_m + Q_m = 0 \quad (\text{A2})$$

Observe that $\partial A_m / \partial \gamma$ can be computed as follows. From Eq. (18) we have

$$\frac{\partial A_m}{\partial \gamma} = \begin{bmatrix} \frac{\partial \hat{A}}{\partial \gamma} & 0 \\ 0 & 0 \end{bmatrix} \quad (\text{A3})$$

and from Eq. (22)

$$\hat{A} M_b = M_b \Lambda_b \quad (\text{A4})$$

Differentiating Eq. (A4) and solving for $d\hat{A}$ we obtain

$$d\hat{A} = dM_b \Lambda_b M_b^{-1} + M_b d\Lambda_b M_b^{-1} - \hat{A} dM_b M_b^{-1} \quad (\text{A5})$$

from which we get either

$$\frac{\partial \hat{A}}{\partial \gamma} = \left(\frac{\partial M_b}{\partial \gamma} \Lambda_b - \hat{A} \frac{\partial M_b}{\partial \gamma} \right) M_b^{-1} \quad (\text{A6})$$

or

$$\frac{\partial \hat{A}}{\partial \gamma} = M_b \frac{\partial \Lambda_b}{\partial \gamma} M_b^{-1} \quad (\text{A7})$$

according to whether γ is a component of μ or of ν . As a consequence of Eq. (23) the entries of $\partial \Lambda_b / \partial \gamma$ are all zero except for a

block. Calling $\partial \Lambda_i / \partial \gamma$ this block, it is found

$$\frac{\partial \Lambda_i}{\partial \gamma} = \begin{bmatrix} \cos \theta_i & \sin \theta_i \\ -\sin \theta_i & \cos \theta_i \end{bmatrix} \quad \text{if } \gamma = \rho_i \text{ and } i \leq \frac{1}{2} n_{im} \quad (\text{A8})$$

$$\frac{\partial \Lambda_i}{\partial \gamma} = \begin{bmatrix} -\rho_i \sin \theta_i & \rho_i \cos \theta_i \\ -\rho_i \cos \theta_i & -\rho_i \sin \theta_i \end{bmatrix} \quad \text{if } \gamma = \theta_i \text{ and } i \leq \frac{1}{2} n_{im} \quad (\text{A9})$$

$$\frac{\partial \Lambda_i}{\partial \gamma} = [1] \quad \text{if } \gamma = \lambda_i \text{ and } i > \frac{1}{2} n_{im} \quad (\text{A10})$$

Vice-versa if γ coincides with the generic entry (say j, k) of M_b , then $\partial M_b / \partial \gamma$ is a matrix with all null elements except for a 1 in position j, k .

Finally, recalling Eq. (21) we obtain

$$\frac{\partial Q_m}{\partial \gamma} = \frac{\partial C_m^T}{\partial \gamma} W_y C_m + C_m^T W_y \frac{\partial C_m}{\partial \gamma} \quad (\text{A11})$$

where, from Eq. (17),

$$\frac{\partial C_m}{\partial \gamma} = \begin{bmatrix} \frac{\partial \hat{C}}{\partial \gamma} & 0 \end{bmatrix} \quad (\text{A12})$$

Recalling that the entries of \hat{C} can be written as linear functions of the entries of \hat{A} , the quantity $\partial \hat{C} / \partial \gamma$ in Eq. (A12) may be evaluated by taking the derivatives of the elements of \hat{C} and using Eqs. (A6) and (A7).

Appendix II: Data Used in Numerical Examples

The numerical examples discussed in the text are based on the following data:

$$\dot{x} = \begin{bmatrix} -0.8060 & 824.2000 \\ -0.0107 & -1.3440 \end{bmatrix} x + \begin{bmatrix} -34.6000 & -37.2000 \\ -4.5720 & -1.2000 \end{bmatrix} u + \begin{bmatrix} 0.8060 & 0 \\ 0.0107 & 0.5034 \end{bmatrix} w_g \quad (\text{B1})$$

$$\dot{d}_g = \begin{bmatrix} -0.9419 & 1.0000 & 0 \\ -0.2218 & 0 & 0 \\ -0.0252 & 0 & -4.5586 \end{bmatrix} d_g + \begin{bmatrix} 1.1887 \\ 0.3232 \\ 0 \end{bmatrix} \eta^g \quad (\text{B2})$$

$$w_g = \begin{bmatrix} 1.0000 & 0 & 0 \\ 0.0055 & 0 & 1 \end{bmatrix} d_g \quad (\text{B3})$$

Matrices C_0 , D_0 , and W_0 are easily computed from Eq. (9) using the eight accelerometer positions in Fig. 1.

References

- ¹Freyman, R., "Interactions Between an Aircraft Structure and Active Control Systems," *Journal of Guidance, Control, and Dynamics*, Vol. 10, No. 5, 1987, pp. 447-452.
- ²Swaim, R. L., Schmidt, D. K., Roberts, P. A., and Hinsdale, A. J., "An Analytical Method for Ride Quality of Flexible Airplanes," *AIAA Journal*, Vol. 15, No. 1, 1977, pp. 4-7.
- ³Swaim, R. L., "Aircraft Elastic Mode Control," *Journal of Aircraft*, Vol. 8, No. 2, 1971, pp. 65-71.
- ⁴Bryson, A. E., Jr., and Ho, Y. C., *Applied Optimal Control*, Hemisphere, Washington, DC, 1975.
- ⁵Bartels, R. H., and Stewart, G. W., "Solution of the Matrix Equation $AX + XB = C$," *Communications of the ACM*, Vol. 15, No. 9, 1972, pp. 820-826.
- ⁶Anon., "Flying Qualities of Piloted Airplanes," MIL-F-8785 C, 1980.
- ⁷Vanderplaats, G. N., *Numerical Optimization Techniques for Engineering Design: With Applications*, McGraw-Hill, New York, 1984, pp. 163-171.
- ⁸Tyler, J. S., Jr., "The Characteristics of Model-Following Systems as Synthesized by Optimal Control," *IEEE Transaction on Automatic Control*, Vol. AC-9, Oct. 1964, pp. 485-498.
- ⁹Kreindler, E., and Rothschild, D., "Model Following in Linear-Quadratic Optimization," *AIAA Journal*, Vol. 14, No. 7, 1976, pp. 835-842.
- ¹⁰Markland, C. A., "Design of Optimal and Suboptimal Stability Augmentation Systems," *AIAA Journal*, Vol. 8, No. 4, 1970, pp. 673-679.
- ¹¹McRuer, D., Ashkenas, I., and Graham, D., *Aircraft Dynamics and Automatic Control*, Princeton University Press, Princeton, N.J., 1973, pp. 307-309.
- ¹²Sadoff, M., Bray, R. S., and Andrews, W. H., "Summary of NASA Research on Jet Transport Control Problems in Severe Turbulence," *Journal of Aircraft*, Vol. 3, No. 3, 1966, pp. 193-200.
- ¹³Kwakernaak, H., and Sivan, R., *Linear Optimal Control Systems*, Wiley, New York, 1972, pp. 427-436.